ACS APPLIED POLYMER MATERIALS

Article

Cite This: ACS Appl. Polym. Mater. 2019, 1, 3304−3312

pubs.acs.org/acsapm

Atmospheric-Pressure Synthesis of Atomically Smooth, Conformal, and Ultrathin Low-*k* Polymer Insulating Layers by Plasma-Initiated Chemical Vapor Deposition

Dominique Abessolo Ondo,[†] François Loyer,[†] Florian Werner,[‡] Renaud Leturcq,[†] Phillip J. Dale,[‡] and Nicolas D. Boscher*[,†]

[†]Materials Research and Technology Department, Luxembourg Institute of Science and Technology, 41, rue du Brill, L-4422 Belvaux, Luxembourg

[‡]Physics and Materials Science Research Unit, University of Luxembourg, 41, rue du Brill, L-4422 Belvaux, Luxembourg

Supporting Information

ABSTRACT: The straightforward synthesis of ultrathin low dielectric constant insulating polymer layers from four cyclic organosilicon monomers (i.e., two organocyclosiloxanes and two organocyclosilazanes) by atmospheric pressure plasma-initiated chemical vapor deposition (AP-PiCVD) is demonstrated. The combination of ultrashort plasma pulses (ca. 100 ns), as polymerization initiator, with long plasma off-times (10 ms), yields the formation of atomically smooth and conformal polymer layers with excellent insulating properties. Leakage current densities of 10^{-9} A cm^{-2} are measured for film thicknesses as low as 12 nm. Low dielectric constants are obtained because of the retention of the cyclic structure of the monomers during the deposition. The polymer layers prepared from 1,3,5,7-tetramethyl-1,3,5,7-tetravinylcyclotrisiloxane display the lowest dielectric constant (k = 2.8). The present study demonstrates the ability to vary the dielectric constant of as-deposited polymer layers by varying the monomer bonds, i.e., siloxane and silazane, as well as their ring size.

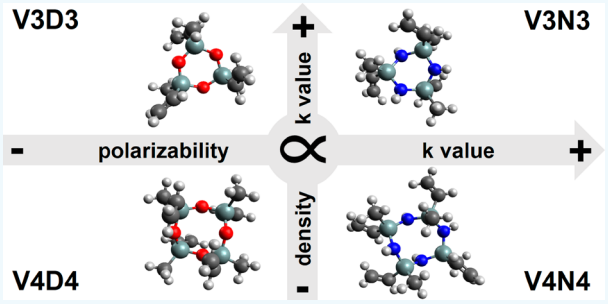

KEYWORDS: *low dielectric constant polymer, polymer dielectric, polymer thin film, atmospheric plasma CVD, plasma-initiated chemical vapor deposition (PiCVD)*

INTRODUCTION

Dielectric polymers are lightweight materials that have attracted a huge interest in electrical and electronic applications because of their insulating properties, chemical resistance, and mechanical flexibility.[1] In particular, dielectric polymer layers have been integrated into various microelectronic devices, including flexible displays[2] and sensors.[2] Integrated into organic field-effect transistors (OFETs) as a gate dielectric, the capacitance (C_i) of these dielectric polymer layers must be kept high enough to ensure a low power operation of the devices.[2] This requirement can be addressed by using polymers with high dielectric constant (denoted ε_r or k). High-k polymers have a low dielectric strength, and thick layers are typically required to prevent high leakage current, ultimately leading to an increase of the power consumption.[3,4] Another strategy is to downscale the thickness of low-k polymer layers.[5,6] The Clausius−Mossotti relation states[7]

$$\frac{\varepsilon_r - 1}{\varepsilon_r + 2} = \frac{N}{3\varepsilon_0}\alpha \quad (1)$$

where ε_r is the material dielectric constant, N is the number of molecules (dipoles) per unit volume (density), and α is the polarizability, which is the sum of the electronic, ionic (also referred to as the distortion[8] or atomic[7] polarization), and orientation (or dipolar[8]) polarizations. Thus, the dielectric constant of polymers can be lowered by doping silicon dioxide using less polarizable bonds, e.g., Si−CH or silicon oxycarbides,[8] and/or decreasing the density (N) via subtractive or constitutive porosities.[8,9]

Solution-based deposition methods, e.g., spin-coating, are broadly employed to deposit low-k polymers in thin film form and are often combined with a thermal curing step to remove the residual solvent.[1,3] Complications appear with the solubility of these polymer layers requiring the use of a cross-linker to prevent a detrimental swelling and implying the use of an orthogonal solvent with underlying layers. Plasma-based processes, broadly used in the microelectronics industry,[9] provide an excellent alternative for the deposition of a wide variety of thin films at both low temperature[10] and atmospheric pressure (AP).[10] A plethora of studies have already reported the plasma-enhanced chemical vapor

Received: August 15, 2019
Accepted: October 25, 2019
Published: October 25, 2019

DOI: 10.1021/acsapm.9b00759
ACS Appl. Polym. Mater. 2019, 1, 3304−3312

deposition (PECVD) of low-k thin films.[10,11] The PECVD of low-k thin films relies on four strategies, i.e., porogen approach,[12] foaming approach,[13] cyclic precursor approach,[14] and carbon-bridging approach,[15] that can be used separately or combined.[14] The two first approaches aim at forming subtractive porosities by thermal,[11] UV, or plasma post-treatments.[16] In addition to the multiplication of the processing steps, subtractive porosity strategies are detrimental to the mechanical properties of the films.[16] On the other hand, constitutive porosity approaches mainly rely on the use of cyclic precursors, e.g., decamethylcyclopentasiloxane (D5),[14] for which a high degree of retention of the ring structure is ensured under mild or pulsed plasma conditions.[15] Nevertheless, minimizing the highly reactive and nonspecific nature of plasma to protect the ring structure of cyclic siloxanes also implies a lower degree of cross-linking of the films.[17] The network connectivity of the films can be increased by introducing carbon-bridging groups.[9] Notably, the use of cyclic siloxanes bearing polymerizable pendant groups, e.g., 1,3,5-trimethyl-1,3,5-trivinylcyclotrisiloxane (V3D3)[15] and 1,3,5,7-tetramethyl-1,3,5,7-tetravinylcyclotrisiloxane (V4D4),[18] promotes a better retention of the ring structure while ensuring the formation of highly cross-linked networks.[15,18] In recent years, the low-pressure-initiated chemical vapor deposition (iCVD) of vinyl-containing cyclosiloxanes has been reported as a convenient alternative to the PECVD approach.[19] iCVD, which can produce ultrathin and conformal polymer insulating layers,[19] is particularly suitable for the preparation of flexible field-effect transistors for low-power soft electronics.[4,5]

However, plasma-based processes still possess significant advantages over iCVD since PECVD can be operated at atmospheric pressure.[10] Moreover, atmospheric plasmas can be implemented as a microplasma torch for the localized deposition and patterning of functional thin films,[10,20] which is particularly relevant to the preparation of semitransparent micro solar cells. Among the developed materials, transparent conductive thin films,[21] crystalline oxide semiconductor thin films,[10,22] and metallic contacts[10,23] can all be formed at low temperature on paper[23] or polymers substrates by using atmospheric plasmas.[21,22] Dielectric layers can also be prepared by using atmospheric plasmas;[24] however, the preparation of ultrathin organic layers with good insulating properties remains a challenge due to the reactivity of plasmas that alters the chemical structure of the monomers and induces particle formation.[14,15] Very recently, the combination of ultrashort plasma pulses (ca. 100 ns) with plasma off-times in the range of the free-radical polymerization lifetime (e.g., 1−100 ms) was demonstrated to yield conformal conventional polymer layers under atmospheric pressure conditions.[25,26] The method, called plasma-initiated chemical vapor deposition, has already been exploited for the atmospheric-pressure deposition of conformal fire-retardant polymer layers on textile,[27] thermoresponsive copolymer layers,[28] and functional polymer layers on 3D substrates for immobilization of biomolecules.[29] The present work aims at investigating further the capabilities of AP-PiCVD in the perspective to extend its range of applications to microelectronics. In particular, this work investigates the ability to form polymer layers with tunable k value by AP-PiCVD. With the objective to decrease of the power consumption of future microelectronic devices, the down-scalability of the dielectric properties of the AP-PiCVD layers is assessed. For the first time, we report the atmospheric-pressure deposition of atomically smooth, conformal, and ultrathin low-k polymer insulating layers from a dry process. The excellent down-scalability of the AP-PiCVD approach is highlighted by the low-leakage current (ca. 10^{-9} A cm^{-2}) measured for a film thickness as low as 12 nm. The high retention of the monomer structure in AP-PiCVD allowed the easy tuning of the k value from the careful selection of the polarizability and ring size of the monomer.

EXPERIMENTAL METHODS

Materials and Substrates. The four investigated monomers, i.e., 1,3,5-trimethyl-1,3,5-trivinylcyclotrisilazane (V3N3), 1,3,5,7-tetravinyl-1,3,5,7-tetramethylcyclotetrasilazane (V4N4), 1,3,5-trivinyl-1,3,5-trimethylcyclotrisiloxane (V3D3), and 1,3,5,7-tetravinyl-1,3,5,7-tetramethylcyclotetrasiloxane (V4D4), were all purchased from Fluorochem and used without any purification. All depositions were carried on intrinsic and highly boron doped (ρ = 0.01 ohm·cm) polished silicon wafers (Siltronix, Archamps, France). Prior to each experiment, the silicon wafers were treated using a 95%/5% argon/oxygen plasma for 40 s. A high-resolution stationary manometer 424-10 (Dwyer, IN) was used to determine the vapor pressure of V3D3, V3N3, V4D4, and V4N4 at 20 °C.

AP-PiCVD of Polymer Layers. The thin films were deposited by using an open-air atmospheric-pressure dielectric barrier discharge setup as previously described.[25] The nanosecond discharges used to initiate the free-radical polymerization of the selected vinylic monomers were ignited by 1 μs square pulses of 6 kV produced by an AHTPB10F generator from EFFITECH, allowing the generation of ultrashort plasma discharges (ca. t_{on} = 100 ns) at a discharge frequency of 100 Hz (i.e., t_{off} = 10 ms). The discharge gap was maintained to 1 mm. Each monomer was directly delivered to the deposition area by using a bubbler setup and argon (Air Liquide, 99.999%) as carrier gas. The flow rate of the argon carrier gas was set to 15 L min^{-1}. The total gas flow was maintained constant to 20 L min^{-1} by using another argon source. To avoid O_2 and N_2 contamination, argon fluxes were added on both sides of the electrodes.

Thin Film Characterizations. Scanning electron microscopy (SEM) images were obtained by using a Hitachi SU-70 FE-SEM. To avoid distortions due to the charge effect, the samples were coated with a 10 nm platinum film prior to the SEM observations. Atomic force microscopy (AFM) images were obtained by using an Innova instrument operating in tapping mode.

Chemical Characterizations. FTIR analyses of the resulting films were performed in reflection mode on Si wafers by using a Bruker Hyperion 2000 spectrometer equipped with an ATR objective. The spectra were obtained over a range of 650−4000 cm^{-1} with a resolution of 4 cm^{-1}. The monomer spectra were acquired with the same FTIR spectrometer. XPS analyses (300 × 700 μm^2) were performed with a Kratos Axis Ultra DLD spectrometer using a monochromatic Al Kα X-ray source ($h\nu$ = 1486.6 eV). A flooding gun was used to reduce charging effect on the samples surface. Photoelectrons emission were collected at 0° angle with respect to the normal. The surface of the samples was precleaned by bombardment with Ar^+ ions (2 kV) and etched for 300 s, prior to the collection of XPS data. Casa XPS software was used for chemical quantification and identification.

Fabrication and Electrical Characterization of the Metal/Insulator/Semiconductor Devices. The synthesized dielectric polymer layers were sandwiched between a highly doped Si wafer used as bottom electrode and a patterned gold layer as top electrode. The patterned gold layers were formed by using shadow masks by electron beam evaporation at a base pressure lower than 10^{-6} mbar. Prior to gold evaporation, a thin layer of titanium (10 nm) was evaporated on top of the AP-PiCVD layers to ensure the adhesion of the gold layer (50 nm). Capacitance versus frequency (C–f) characteristics of the metal/insulator/semiconductor (MIS) devices were measured by using an impedance analyzer (IM 3570 HIOKI). The C–f measurements were performed in a range of frequencies

DOI: 10.1021/acsapm.9b00759
ACS Appl. Polym. Mater. 2019, 1, 3304−3312

from 100 Hz to 1 MHz with an excitation level of 0.1 V. The $J-V$ characteristic measurements of the MIS devices were performed at ambient atmosphere by using a Keithley 2614B instrument while the voltage was from −20 to 20 V.

Density Functional Theory (DFT) Calculations. DFT calculations were performed by using the 4.0.1 program suite using the HPC facilities of the University of Luxembourg.[30,31] The hybrid functional B3LYP was used for every calculation along with Ahlrichs' basis set def2-TZVP and Weighend's auxiliary basis set def2/J.[32,33] The numerical chain of sphere approximation RIJCOSX and the dispersion correction D3 were also applied in any instance.[34,35] The bond dissociation energies (BDE) of the investigated monomers were calculated by using a previously reported method.[26] Analytical frequency calculations were performed for each fragment and molecule to obtain their free enthalpy and to ensure the convergence of the calculation. Because of the molecules' symmetry, only a third (for V3N3 and V3D3) and fourth (for V4N4 and V4D4) of the BDE were calculated and reported.

RESULTS AND DISCUSSION

AP-PiCVD of Atomically Smooth and Conformal Ultrathin Polymer Layers. To demonstrate our atmospheric-pressure chemical vapor deposition approach toward the simultaneous synthesis and deposition of atomically smooth, conformal, and ultrathin insulating polymer layers with tunable dielectric properties, four different cyclic monomers were selected, i.e., two silazanes (1,3,5-trimethyl-1,3,5-trivinylcyclotrisilazane (V3N3) and 1,3,5,7-tetravinyl-1,3,5,7-tetramethylcyclotetrasilazane (V4N4)) as well as two siloxanes (1,3,5-trivinyl-1,3,5-trimethylcyclotrisiloxane (V3D3) and 1,3,5,7-tetravinyl-1,3,5,7-tetramethylcyclotetrasiloxane (V4D4)). Briefly, they are six- to eight-member silazane or siloxane rings with three to four vinyl pendant groups, respectively (Figure 1). The vinyl groups are a prerequisite in AP-PiCVD, which relies on the free-radical polymerization reaction.[26,36] The cyclic structure of the selected monomers is foreseen to provide a constitutive porosity to the polymer layers and therefore yield a low dielectric constant according to the Clausius−Mossotti equation (eq 1).[7] Thus, the four monomers, which differ by their polarizability, i.e., different chemical bonds between the silazanes and siloxanes, and/or their ring sizes (Figure 1), should yield different dielectric constants. The pore surface area of each siloxane and silazane rings was determined in their most stable geometry by DFT calculations. The silazane's pores are roughly 6% larger than the siloxane's ones due to longer Si−N (174 pm) bonds in comparison to Si−O (166 pm) bonds and lower Si−N−Si (106−110° and 122−128°) angles in comparison to the Si−O−Si (109−110° and 131−143°) angles. In a general manner, the pore surface area increases by 40% when increasing the ring members from six (i.e., V3D3 and V3N3) to eight (i.e., V4D4 and V4N4).

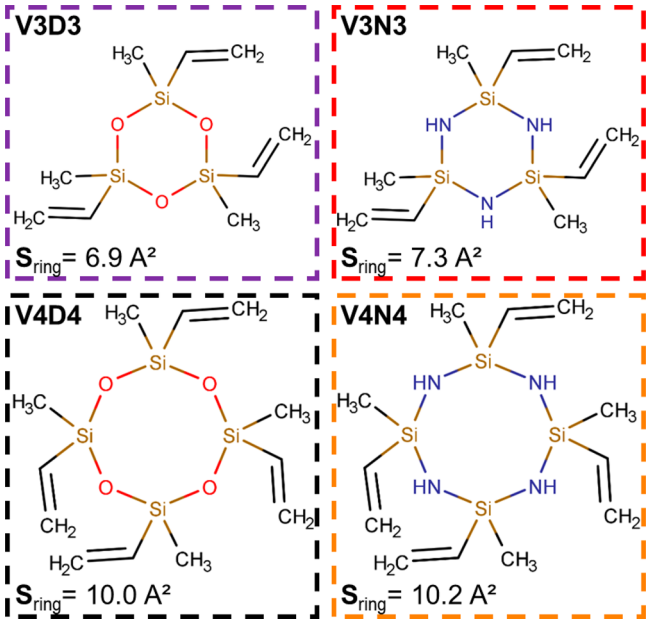

Figure 1. Chemical structure of the V3D3, V3N3, V4D4, and V4N4 monomers. The DFT calculated ring size of these cyclic monomers ranges from 6.9 Å^2 to 7.3, 10.0, and 10.2 Å^2 for V3D3, V3N3, V4D4, and V4N4, respectively.

To initiate the free-radical polymerization of the selected monomers, we employed 1 μs square-wave high-voltage pulses (6 kV) to ignite an atmospheric-pressure dielectric barrier discharge in argon (Figure 2a). Each high-voltage pulse

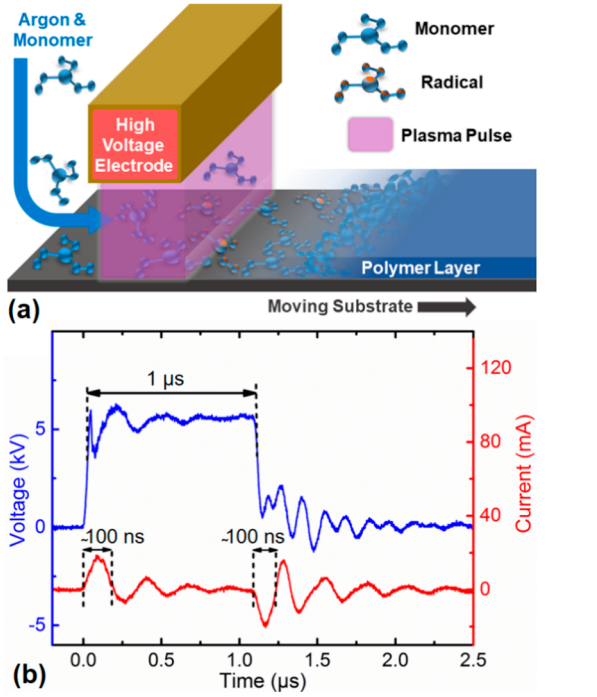

Figure 2. (a) Scheme of the atmospheric-pressure plasma-initiated chemical vapor deposition used for the preparation of atomically smooth, conformal, and ultrathin low-k polymer insulating layers. (b) Traces of the high-voltage pulse and current discharges.

generates two distinct current discharges (ca. 100 ns) at the voltage rising and falling edges (Figure 2b). The repetition frequency of the high-voltage pulses was set to 100 Hz. This corresponds to a 10 ms plasma off-time, which is consistent with the lifetime of the free-radical polymerization reaction of vinyl compounds in AP-PiCVD.[25,27,28,36]

The AP-PiCVD reaction of the selected monomers leads to the deposition of macroscopically smooth and defect-free thin films across the entire surface of the substrates, including 4 in. silicon wafers. Scanning electron microscopy (SEM) observations confirmed that, irrespective of the monomers, smooth and particle-free thin films are formed over the whole surface of the substrate (Supporting Information Figure S1). The pinhole-free nature and low particulate density of the AP-

DOI: 10.1021/acsapm.9b00759
ACS Appl. Polym. Mater. 2019, 1, 3304−3312

PiCVD thin films are further confirmed through atomic force microscopy (AFM) investigations (Figure 3). More importantly, AFM highlights the atomically smooth nature of the AP-PiCVD thin films with a root-mean-squared roughness (R_q) measured below 7 Å, even for thicknesses higher than 300 nm (Figure 3). Such low R_q values, similar to the ones measured for the thin films grown by low-pressure iCVD,[37] make the proposed AP-PiCVD approach highly suitable for OTFT applications.[2]

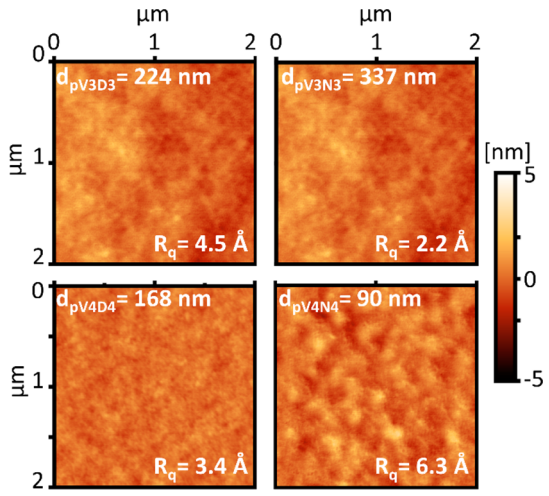

Figure 3. Atomic force microscopy (AFM) images and root-mean-square roughness (R_q) of pV3D3 (d = 224 nm), pV4D4 (d = 168 nm), pV3N3 (d = 377 nm), and pV4N4 (d = 126.7 nm) coatings prepared by AP-PiCVD. d is the thickness of the thin films.

SEM cross-sectional observation of the AP-PiCVD thin films deposited on a trenched wafer highlights their excellent conformality with a d_{bottom}/d_{top} and a $d_{sidewall}/d_{top}$ ratio close to 100% and 63%, respectively (Figure 4). d_{top}, $d_{sidewall}$, and d_{bottom} are the thicknesses at the top, sidewall, and bottom of the trench, respectively. The conformal coverage of 3-dimensional structures, which is very difficult to achieve by classical wet methods, is also highly desirable for the preparation of functional devices, e.g., sensors[38] and transistors.[5]

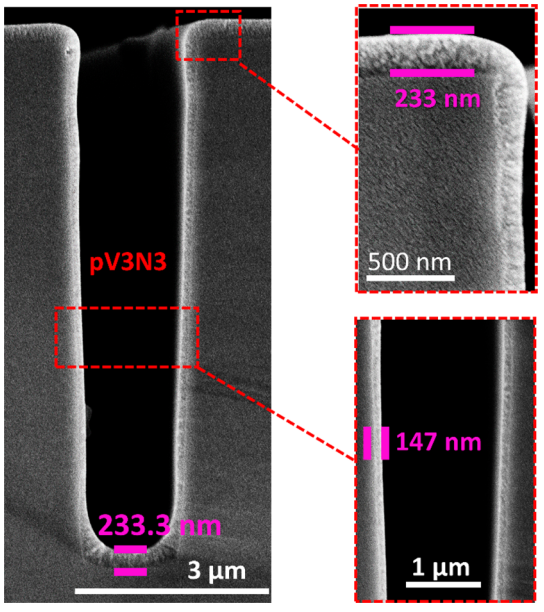

Figure 4. SEM cross-sectional image of 233 nm thick pV3N3 coating on a 9 μm deep and 1.5 μm wide silicon trench structure.

In addition to the atomically smooth and conformal nature of the as-deposited layers, the AP-PiCVD process allowed their rather fast and uniform deposition. Ellipsometry measurements confirmed that uniform thicknesses were achieved across the whole length of the silicon substrates. The deposition rates were evaluated to be 0.68, 0.70, 0.96, and 0.42 nm s^{-1} for the V3D3, V3N3, V4D4, and V4N4 monomers, respectively (Table 1). The monomer carrier gas flow (15 slm), in which the monomer partial pressure (P_M) is approximately its vapor pressure (P_{sat}), and dilution flow (5 slm) being identical for the four monomers, the P_M/P_{sat} ratio was constant for all monomers (in spite of their different P_{sat}).[39] This approach ensures comparable adsorption mechanisms that are known to have a strong influence on the growth mechanisms in the AP-PiCVD process.[26,36] The slight growth rate differences can be attributed to different polymerization rate parameters.[36] First, the different P_{sat} of the monomers (Table 1) for a constant P_M/P_{sat} ratio implies different monomer gas phase concentrations that directly affect the amount of initiating species [M$^\bullet$] and the initiation rate R_i. One can also assume that the four monomers possess different propagation constants (k_p) that yield different propagation rates (R_p). In other words, in a process driven by surface reactions where a comparable amount of monomer adsorbs $[M]_{ad}$ on the surface, the growth rates are determined by the ability of the adsorbed monomer to polymerize prior to its desorption.

Table 1. Vapor Pressure (P_{sat}), Deposition Rate (DR), Pore Size, and k Value of the V3D3, V3N3, V4D4, and V4N4 Monomers and Their Respective As-Deposited AP-PiCVD Layers

monomer	P_{sat} (Torr)	DR (nm s^{-1})	pore size (Å^2)	k
V3D3	3.33	0.69 ± 0.09	6.9	3.6 ± 0.1
V3N3	>18	0.70 ± 0.04	7.3	4.2 ± 0.1
V4D4	0.04	0.96 ± 0.04	10.0	2.8 ± 0.1
V4N4	0.29	0.42 ± 0.04	10.2	3.7 ± 0.1

The AP-PiCVD thin films were soaked for 24 h in different solvents to investigate their chemical stability. After 24 h immersion in common polar solvents, i.e., acetone and ethanol, the thickness of the layers was unaltered for the pV4D4 and pV4N4 layers and only slightly reduced (ca. 8 to 20%) for the pV3D3 and pV3N3 layers (Table S1 and Figure S2). More interestingly, the organosilicon layers retain their atomically smooth nature with a Rq measured below 10 Å, which is desirable for application in microelectronic. These observations underline the excellent chemical stability of the organosilicon layers and suggest the successful polymerization of the vinyl pendant groups of studied monomers, yielding highly cross-linked organosilicon networks.

Ultrathin Low-*k* Polymer Insulating Layer. A series of metal/insulator/semiconductor (MIS) structures were fabricated to evaluate the dielectric properties of the as-deposited polymer layers (Table S2). All the polymer layers deposited from V3N3, V4D4, and V4N4 (pV3N3, pV4D4, and pV4N4) were able to sustain a voltage up to 20 V without any occurrence of an electrical breakdown, even for thicknesses as low as 12 nm (Figure 5). Additional measurements performed

DOI: 10.1021/acsapm.9b00759
ACS Appl. Polym. Mater. 2019, 1, 3304−3312

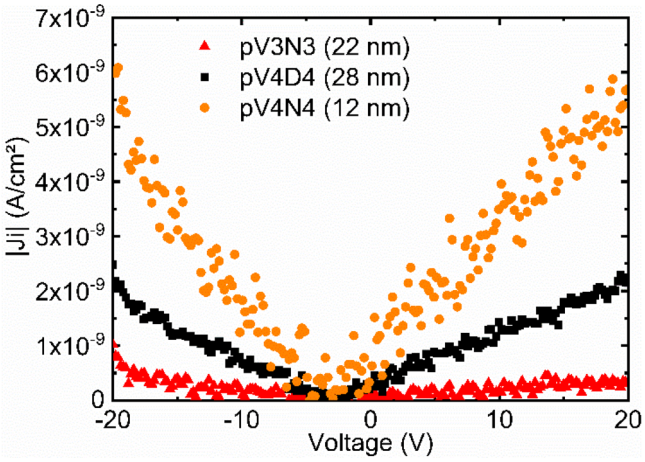

Figure 5. Voltage dependence of the absolute leakage current density $|J_i(V)|$ of the MIS devices with the ultrathin (d < 30 nm) AP-PiCVD layers grown from V3N3, V4D4, and V4N4.

on thicker polymer layers are available in Figure S3. For all the presented polymers layers, the experimental current−voltage characteristics show a linear behavior indicating an ohmic leakage current. The apparent increase of the measured current around −20 V was attributed to a transient response when abruptly applying the bias voltage at the beginning of the measurement. Thus, the initial data points (V < −17 V) have been disregarded for the analysis. The linear fits of the experimental current−voltage characteristics (solid lines in Figure S3) reveal resistance values in a range of approximately 4−55 GΩ cm^2 for different pV3N3, pV4D4, and pV4N4 layers. Taking into account the thickness of the polymer layers, these effective resistance values correspond to specific resistivities of $\rho = (4 \pm 2) \times 10^{15}$ Ω cm for pV4D4 and pV4N4 and slighly higher values of 10^{16} Ω cm and more for pV3N3. Such excellent insulation properties highlight the ability of our low-frequency ultrashort plasma pulses approach, i.e., AP-PiCVD, to produce insulating ultrathin dielectric layers under atmospheric pressure conditions in an open-air reactor. These excellent insulating properties were confirmed with leakage current densities (J_i) below 10^{-8} A cm^{-2} for the AP-PiCVD layers grown from V3N3, V4D4, and V4N4 (Figure S3), making them attractive as gate dielectric polymers. Surprisingly, an electrical breakdown, which is defined as an exponential increase of the leakage current density,[2] was observed for rather low electrical field for the pV3D3 layers (Figure S4). Indeed, for 23 nm thick pV3D3 layer, a voltage of 4.6 V yields to an abrupt increase of J_i, corresponding to a breakdown electric field (E_b) of 1.5 MV cm^{-1}. This early dielectric breakdown observed for the pV3D3 layers may find its origin in the much higher saturation pressure (P_{sat}) of the V3D3 monomer (Table 1). Indeed, with the aim of making fair comparisons between the four monomers selected, identical argon carrier gas flows (15 L min^{-1}) have been used with the aim to investigate a similar P_M/P_{sat} ratio (approximated to be equal to the ratio of the carrier gas flow rate over the total flow rate). Therefore, the much higher P_{sat} of V3D3 implies a much higher partial pressure (P_M) of this monomer that may either be responsible of a partial quenching of the nanosecond

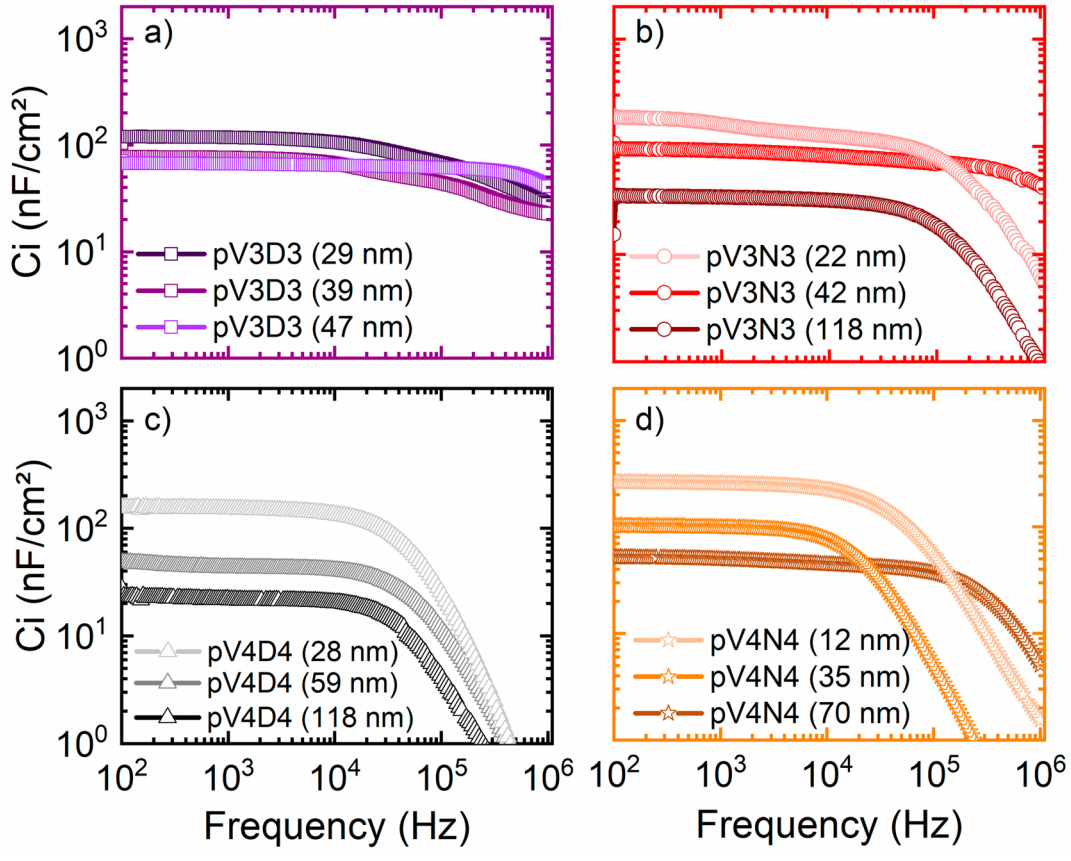

Figure 6. C_i versus frequency of all the as-deposited (a) pV3D3, (b) pV3N3, (c) pV4D4, and (d) pV4N4 layers with various thicknesses.

DOI: 10.1021/acsapm.9b00759
ACS Appl. Polym. Mater. 2019, 1, 3304−3312

discharges or promote the formation of smaller oligomers[25] that could altered the dielectric resistance of the films.

For each of the investigated monomers, the areal capacitance (C_i) of all the as-deposited polymer layers was systematically measured on three samples of different thickness and plotted with respect to the frequency (Figure 6). An abrupt drop of the capacitance with vanishing capacitance in the high frequency limit was observed for the pV3N3, pV4D4, and pV4N4 layers, while the pV3D3 and pV3N3 (42 nm) layers show smaller capacitance steps. Such capacitance steps might, for example, be related to defects in the films, parasitic capacitances, or a dipole orientation lag of the molecule behind the alternating electric field, commonly termed the polarization effect.[4] The pronounced high frequency drop of the capacitance down to zero is instead attributed to the series resistance of the MIS structure[40] because the measured capacitance drops below the minimum geometric capacitance $C_0 = \varepsilon_0/d_{polymer}$.

The real part of the dielectric constant ($\varepsilon' = k$) of each polymer layer was estimated from the relation

$$C_i = \frac{\varepsilon_0 \varepsilon'_{polymer}}{d_{polymer}} \quad (2)$$

where C_i was measured at 1 kHz for different layer thicknesses (Figure 7). It is noteworthy to underline that the C_i of all the

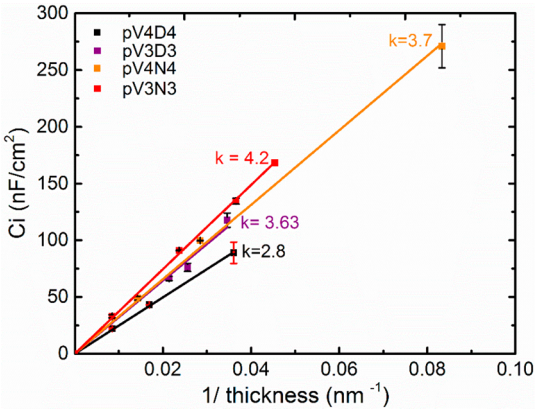

Figure 7. Estimation of the dielectric constant of the as-deposited pV3D3, pV3N3, pV4D4, and pV4N4 layers.

synthesized layers was stable in the studied frequency range, i.e., low frequencies. The siloxane layers exhibited the lowest dielectric constant compared to the silazane ones, i.e., k_{pV3D3} = 3.6 ± 0.1 and k_{pV4D4} = 2.8 ± 0.1. It should be highlighted here that the k_{pV4D4} value (2.8) is in accordance with the values reported for the pV4D4 layers prepared from the low-pressure-initiated chemical vapor deposition method, i.e., k = 2.8 ± 0.1.[41] On the other hand, the k values of the pV3N3 and pV4N4 layers were evaluated to 4.2 ± 0.1 and 3.7 ± 0.1, respectively. While the dense silicon dioxide (SiO_2) has a k_{SiO_2} = 4.0 ± 0.1,[8] the silicon carbonitride (SiC_xN_y) has a $k_{SiC_xN_y}$ = 4.5−5.5.[42] Consequently, the low dielectric constant ($k < 4$)[39] of the pV3D3, pV4D4, and pV4N4 must stem from the ability of the AP-PiCVD process to preserve the ring's structure of the selected monomers.

The FTIR spectra of the as-deposited polymer layers (Figure 8) confirmed the assumption of the preservation of the ring's structure responsible for the low dielectric constants measured. Indeed, all the polymer layers exhibit strong similarities with their respective monomer (Tables S3−S6), whereas the qualitative reduction (pV3D3 and pV3N3) or full disappearance (pV4D4 and pV4N4) of the absorbance peaks of vinyl bond located at ca. 1600 cm^{-1} and ca. 3050 cm^{-1} suggests the predominance of the free-radical polymerization pathway (Figure 8 and Figure S5).

The strong absorbance peak corresponding to the cyclic siloxane ring of V4D4 located at 1053 cm^{-1} is present in both the spectra of the monomer and the polymer layer (Figure 8c). The absence of broadening of this peak for the polymer layer is consistent with the hypothesis that the AP-PiCVD process has preserved the original cyclic siloxane ring of V4D4. Similarly, the strong absorption peak observed in the both spectra of V3D3 and the as-deposited pV3D3 layers at 997 cm^{-1} (corresponding to the Si−O—Si tricyclosiloxane ring) points out a fair retention of the tricyclosiloxane ring during the deposition. However, the presence of a weak peak that can be attributed to Si——O open cycle moieties can also be observed around 1080 cm^{-1}.[41] Ring-opening of cyclic monomers is not surprising and can be attributed to plasma-induced side reactions. This can justify the higher dielectric constant of the formed pV3D3 layers (3.6) compared to the one synthesized by iCVD, i.e., k^{iCVD}_{pV3D3} = 2.2.[5] On the other hand, FTIR suggests a retention of the other groups in the pV3D3 layers, notably the methyl and ethyl groups bonded to silicon (Figure S6). The mono-, di-, or trisubstitution of the silicon atom with oxygen, designated as "M", "D", and "T" configurations, respectively, can be easily monitored from the Si−CH_3 symmetric bending peak observed in the 1300−1240 cm^{-1} region (Figure S6). Shifting of this absorption peak toward higher wavenumbers is indicative of a higher substitution of carbon by oxygen atoms (O_x−Si−$(CH_3)_{4-x}$ with x = 1, 2, 3).[15,43] Despite the possible ring-opening of V3D3 during the deposition process, the original D configuration of the silicon was retained. This result further confirms the prevalence of the free-radical polymerization reaction over the opening of the V3D3 ring. To understand the reactivity difference between the V3D3 and V4D4 in AP-PiCVD, DFT calculation of their bond dissociation energies (BDE) was performed and pointed out the weaker stability of the Si−O bonds of V3D3 (4.0 eV) compared those of V4D4 (5.5 eV) (Figure S7). Thus, the differences in energy of the Si−O bonds with the other single σ-bonds in V4D4 are significant (ΔBDE ≈ 1.5 eV) and suggest a much lower sensitivity of the cyclotetrasiloxane ring to plasma breakdown, while the cyclotrisiloxane ring is not granted any protection due to the rather small differences in energy with the other single σ-bonds present in V3D3 (ΔBDE < 0.2 eV).

The FTIR spectra of the layers elaborated from V3N3 and V4N4 both exhibit a broad peak between 930 and 1140 cm^{-1} (Figure 8b,d), which differs from the sharp Si−N−Si peaks of the silazane rings of their respective monomers observed at ca. 930−910 and 1005 cm^{-1} (Tables S4 and S6).[37,44] Moreover, the peaks related to the stretching and deformation of N−H at 3399 and 1155 cm^{-1}, respectively, disappear. Such a broadening or disappearance of the peaks is consistent with the observation made for the pV3N3 and pV4N4 coatings elaborated by iCVD.[37] Moreover, these observations contrast with the ones made for PECVD coatings where N−H bands increase due to the disruption of the silazane rings.[44] Nevertheless, the FTIR spectra of the layers elaborated from V3N3 and V4N4 also strongly resemble the ones obtained for pV3D3 and pV4D4 (Figure 8), and the enlargement of the Si−

DOI: 10.1021/acsapm.9b00759
ACS Appl. Polym. Mater. 2019, 1, 3304−3312

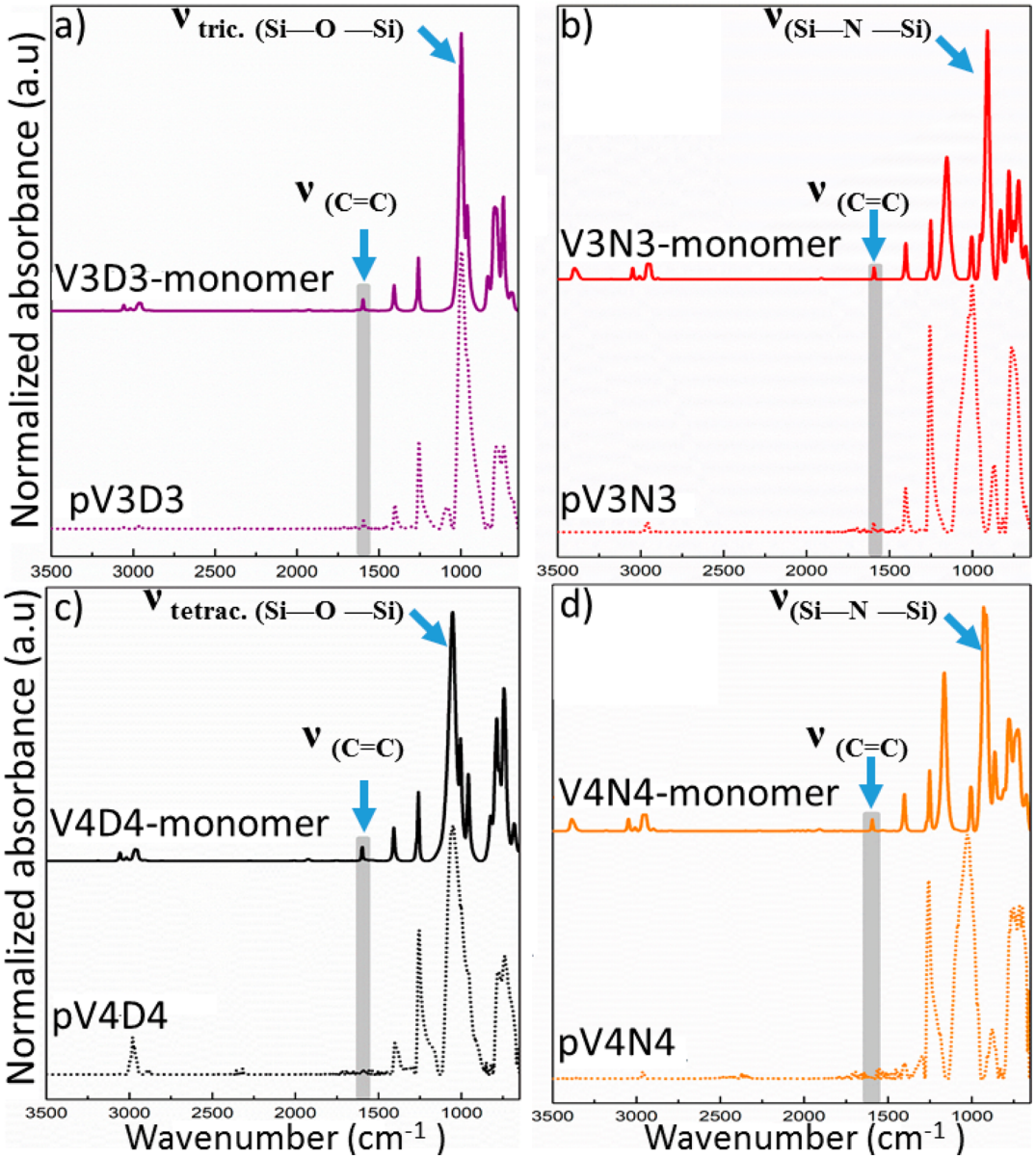

Figure 8. FTIR spectra of the AP-PiCVD layers synthesized from (a) V3D3, (b) V3N3, (c) V4D4, and (d) V4N4 and their respective monomers.

N−Si peaks between 930 and 1140 cm^{-1} could be related to the formation of Si−O−Si bonds when operating under open-atmosphere conditions. One should also mention the shift of the Si−CH_3 peak of the silazane-based coatings to higher wavenumbers, i.e., from 1252 to 1257 cm^{-1}, indicative of a partial oxidation of silicon (Figure S6). Therefore, a quantitative XPS analysis of the chemical composition of the AP-PiCVD coatings was undertaken to evidence any discrepancy between the expected and actual chemical compositions of the films. Unsurprisingly in view of their FTIR spectra, the pV3D3 and pV4D4 layers exhibit an almost perfect match with their expected chemical composition (Table S7). On the other hand, XPS analysis of the layers obtained from V3N3 and V4N4 reveals a drastic decrease of the nitrogen content, from 20% expected to ca. 0.6−10% measured, coupled with the incorporation of oxygen, ca. 19% (Table S7). Hence, the broadening of the Si−N−Si peaks observed in the FTIR spectra of the layers obtained from the silazane monomers can be attributed to the oxidation of silicon and the formation of Si−O bonds, in accordance with previous PECVD studies.[45]

It is noteworthy to highlight that for all the investigated monomers the formation and incorporation of −OH groups was not detected in the AP-PiCVD coatings. Indeed, the presence of a hydroxyl group was not observed by FTIR, neither at 3500 cm^{-1} nor at 920−830 cm^{-1}.[15] This aspect is important for the targeted application since the sorption of water in the dielectric layer should be avoided because the inclusion of such highly polarizable bonds −OH would lead to an increase in the resulting k value. Overall, the lower bond polarizability of the siloxane compounds and the larger and more stable ring of V4D4 make it the monomer of choice to grow ultrathin low-k polymer insulating layers by AP-PiCVD. Such findings could considerably simplify the elaboration of microelectronic devices.

DOI: 10.1021/acsapm.9b00759
ACS Appl. Polym. Mater. 2019, 1, 3304−3312

CONCLUSION

Atomically smooth, conformal, and ultrathin low-k polymer insulating layers were successfully deposited from a straightforward atmospheric-pressure gas phase approach based on ultrashort plasma pulses. The polymer layers, prepared from various cyclic organosilicon monomers (V3N3, V4D4, and V4N4), showed excellent insulating properties with a leakage current density of 10^{-9} A cm^{-2} for layers as thin as 12 nm. These excellent insulating properties have been attributed to the pinhole and defect-free nature of the organosilicon films. The ability to vary the dielectric constant of the resulting polymer layers was achieved by varying the polarizability of the monomer bonds, i.e., siloxane and silazane, as well as the monomer ring size. Particularly, the cyclic siloxane layers exhibited lower dielectric constant values (k_{pV3D3} = 3.6 and k_{pV4D4} = 2.8) compared to the cyclic silazane layers (k_{pV3N3} = 4.2 and k_{pV4N4} = 3.7) due to the lower polarizability of the siloxane bonds. The retention of the ring structure in AP-PiCVD allowed the synthesis of polymer layers bearing a constitutive porosity, with the layers elaborated from the larger siloxane ring (V4D4) possessing the lowest dielectric constant values (k_{pV4D4} = 2.8).

ASSOCIATED CONTENT

Supporting Information

The Supporting Information is available free of charge on the ACS Publications website at DOI: 10.1021/acsapm.9b00759.

SEM of the organosilicon-based coatings, thickness, and roughness variation of the organosilicon-based coatings after soaking in common solvents, list and characteristics of the organosilicon-based coatings integrated in MIS devices, voltage dependence of the leakage current density for the organosilicon-based coatings, assignation of the FTIR peaks for the organosilicon-based coatings and their respective monomer, enlargement of the main FTIR peaks of interest, bond dissociation energies for the investigated monomers and XPS quantification of the organosilicon-based coatings (PDF)

AUTHOR INFORMATION

Corresponding Author

*Phone: +352 275 888 578. E-mail: nicolas.boscher@list.lu.

ORCID

Florian Werner: 0000-0001-6901-8901
Renaud Leturcq: 0000-0001-7115-9172
Nicolas D. Boscher: 0000-0003-3693-6866

Notes

The authors declare no competing financial interest.

ACKNOWLEDGMENTS

The Luxembourg National Research Fund (FNR) is thanked for financial support through the MASSENA project (PRIDE15/10935404). We thank Dr. J. Guillot, Dr. S. Girod, and P. Grysan for the acquisition of the XPS data, the MIS preparation, and AFM measurements. Dr. M. Guennou, Dr. K. Baba, G Bengasi, and P. Baustert are acknowledged for insightful discussions. The DFT calculations presented in this paper were performed using the HPC facilities of the University of Luxembourg.

REFERENCES

(1) Maier, G. Low Dielectric Constant Polymers for Microelectronics. *Prog. Polym. Sci.* **2001**, *26*, 3−65.
(2) Wang, B.; Huang, W.; Chi, L.; Al-Hashimi, M.; Marks, T. J.; Facchetti, A. High- k Gate Dielectrics for Emerging Flexible and Stretchable Electronics. *Chem. Rev.* **2018**, *118*, 5690−5754.
(3) Yoon, M. H.; Yan, H.; Facchetti, A.; Marks, T. J. Low-Voltage Organic Field-Effect Transistors and Inverters Enabled by Ultrathin Cross-Linked Polymers as Gate Dielectrics. *J. Am. Chem. Soc.* **2005**, *127*, 10388−10395.
(4) Choi, J.; Joo, M.; Seong, H.; Pak, K.; Park, H.; Park, C. W.; Im, S. G. Flexible, Low-Power Thin-Film Transistors Made of Vapor-Phase Synthesized High-k, Ultrathin Polymer Gate Dielectrics. *ACS Appl. Mater. Interfaces* **2017**, *9*, 20808−20817.
(5) Moon, H.; Seong, H.; Shin, W. C.; Park, W.-T.; Kim, M.; Lee, S.; Bong, J. H.; Noh, Y.-Y.; Cho, B. J.; Yoo, S.; Im, S. G. Synthesis of Ultrathin Polymer Insulating Layers by Initiated Chemical Vapour Deposition for Low-Power Soft Electronics. *Nat. Mater.* **2015**, *14*, 628−635.
(6) Ortiz, P.; Facchetti, A.; Marks, T. J. High- k Organic, Inorganic, and Hybrid Dielectrics for Low-Voltage Organic Field-Effect Transistors. *Chem. Rev.* **2010**, *110*, 205−239.
(7) Ku, C. C.; Liepins, R. *Electrical Properties of Polymers: Chemical Principles*; Hanser Gardner Publications: 1987.
(8) Maex, K.; Baklanov, M. R.; Shamiryan, D.; Iacopi, F.; Brongersma, S. H.; Yanovitskaya, Z. S. Low Dielectric Constant Materials for Microelectronics. *J. Appl. Phys.* **2003**, *93*, 8793−8841.
(9) Volksen, W.; Miller, R. D.; Dubois, G. Low Dielectric Constant Materials. *Chem. Rev.* **2010**, *110*, 56−110.
(10) Mariotti, D.; Belmonte, T.; Benedikt, J.; Velusamy, T.; Jain, G.; Švrček, V. Low-Temperature Atmospheric Pressure Plasma Processes for "Green" Third Generation Photovoltaics. *Plasma Processes Polym.* **2016**, *13*, 70−90.
(11) You, H.; Mennell, P.; Shoudy, M.; Sil, D.; Dorman, D.; Cohen, S.; Liniger, E.; Shaw, T.; Leo, T.-L.; Canaperi, D.; Raymond, M.; Madan, A.; Grill, A. Extreme-Low k Porous PSiCOH Dielectrics Prepared by PECVD. *J. Vac. Sci. Technol., B: Nanotechnol. Microelectron.: Mater., Process., Meas., Phenom.* **2018**, *36*, 012202.
(12) Jousseaume, V.; Favennec, L.; Zenasni, A.; Gourhant, O. Porous Ultra Low k Deposited by PECVD: From Deposition to Material Properties. *Surf. Coat. Technol.* **2007**, *201*, 9248−9251.
(13) El Sabahy, J.; Castellan, G.; Ricoul, F.; Jousseaume, V. Porous SiOCH Thin Films Obtained by Foaming. *J. Phys. Chem. C* **2016**, *120*, 9184−9191.
(14) Castex, A.; Favennec, L.; Jousseaume, V.; Bruat, J.; Deval, J.; Remiat, B.; Passemard, G.; Pons, M. Study of Plasma Mechanisms of Hybrid A-SiOC:H Low-k Film Deposition from Decamethylcyclopentasiloxane and Cyclohexene Oxide. *Microelectron. Eng.* **2005**, *82*, 416−421.
(15) Burkey, D. D.; Gleason, K. K. Structure and Mechanical Properties of Thin Films Deposited from 1,3,5-Trimethyl-1,3,5-Trivinylcyclotrisiloxane and Water. *J. Appl. Phys.* **2003**, *93*, 5143−5150.
(16) Gourhant, O.; Gerbaud, G.; Zenasni, A.; Favennec, L.; Gonon, P.; Jousseaume, V. Crosslinking of Porous SiOCH Films Involving Si-O-C Bonds: Impact of Deposition and Curing. *J. Appl. Phys.* **2010**, *108*, 124105.
(17) Jousseaume, V.; El Sabahy, J.; Yeromonahos, C.; Castellan, G.; Bouamrani, A.; Ricoul, F. SiOCH Thin Films Deposited by Chemical Vapor Deposition: From Low-k to Chemical and Biochemical Sensors. *Microelectron. Eng.* **2017**, *167*, 69−79.
(18) Lubguban, J.; Rajagopalan, T.; Mehta, N.; Lahlouh, B.; Simon, S. L.; Gangopadhyay, S. Low-k organosilicate films prepared by tetravinyltetramethylcyclotetrasiloxane. *J. Appl. Phys.* **2002**, *92*, 1033−1038.
(19) Wang, M.; Wang, X.; Moni, P.; Liu, A.; Kim, D. H.; Jo, W. J.; Sojoudi, H.; Gleason, K. K. CVD Polymers for Devices and Device Fabrication. *Adv. Mater.* **2017**, *29*, 1604606.

DOI: 10.1021/acsapm.9b00759
ACS Appl. Polym. Mater. 2019, 1, 3304−3312

(20) Belmonte, T.; Henrion, G.; Gries, T. Nonequilibrium Atmospheric Plasma Deposition. *J. Therm. Spray Technol.* **2011**, *20*, 744−759.
(21) Abessolo Ondo, D.; Loyer, F.; Chemin, J. B.; Bulou, S.; Choquet, P.; Boscher, N. D. Atmospheric Plasma Oxidative Polymerization of Ethylene Dioxythiophene (EDOT) for the Large-Scale Preparation of Highly Transparent Conducting Thin Films. *Plasma Processes Polym.* **2018**, *15*, 1700172.
(22) Quesada-González, M.; Baba, K.; Sotelo-Vázquez, C.; Choquet, P.; Carmalt, C. J.; Parkin, I. P.; Boscher, N. D. Interstitial boron-doped anatase TiO_2 thin-films on optical fibres: atmospheric pressure-plasma enhanced chemical vapour deposition as the key for functional oxide coatings on temperature-sensitive substrates. *J. Mater. Chem. A* **2017**, *5*, 10836−10842.
(23) Knapp, C. E.; Chemin, J.-B.; Douglas, S. P.; Abessolo Ondo, D.; Guillot, J.; Choquet, P.; Boscher, N. D. Room-Temperature Plasma-Assisted Inkjet Printing of Highly Conductive Silver on Paper. *Adv. Mater. Technol.* **2018**, *3*, 1700326.
(24) Park, J.; Cho, N.-K.; Lee, S.-E.; Lee, E. G.; Lee, J.; Im, C.; Na, H.-J.; Kim, Y. S. Atmospheric-pressure plasma treatment toward high-quality solution-processed aluminum oxide gate dielectric films in thin-film transistors. *Nanotechnology* **2019**, *30*, 495702.
(25) Loyer, F.; Frache, G.; Choquet, P.; Boscher, N. D. Atmospheric Pressure Plasma-Initiated Chemical Vapor Deposition (AP-PiCVD) of Poly(Alkyl Acrylates): An Experimental Study. *Macromolecules* **2017**, *50*, 4351−4362.
(26) Loyer, F.; Bengasi, G.; Frache, G.; Choquet, P.; Boscher, N. D. Insights in the Initiation and Termination of Poly(Alkyl Acrylates) Synthesized by Atmospheric Pressure Plasma-Initiated Chemical Vapor Deposition (AP-PiCVD). *Plasma Processes Polym.* **2018**, *15*, 1800027.
(27) Hilt, F.; Boscher, N. D.; Duday, D.; Desbenoit, N.; Levalois-Grützmacher, J.; Choquet, P. Atmospheric pressure plasma-initiated chemical vapor deposition (AP-PiCVD) of poly-(diethylallylphosphate) coating: A char-forming protective coating for cellulosic textile. *ACS Appl. Mater. Interfaces* **2014**, *6*, 18418−18422.
(28) Loyer, F.; Combrisson, A.; Omer, K.; Moreno-Couranjou, M.; Choquet, P.; Boscher, N. D. Thermoresponsive Water-Soluble Polymer Layers and Water-Stable Copolymer Layers Synthesized by Atmospheric Plasma Initiated Chemical Vapor Deposition. *ACS Appl. Mater. Interfaces* **2019**, *11*, 1335−1343.
(29) Bonot, S.; Mauchauffé, R.; Boscher, N. D.; Moreno-Couranjou, M.; Cauchie, H.-M.; Choquet, P. Self-Defensive Coating for Antibiotics Degradation - Atmospheric Pressure Chemical Vapor Deposition of Functional and Conformal Coatings for the Immobilization of Enzymes. *Adv. Mater. Interfaces* **2015**, *2*, 1500253.
(30) Neese, F. The ORCA Program System. *WIREs Comput. Mol. Sci.* **2012**, *2*, 73−78.
(31) Varrette, S.; Bouvry, P.; Cartiaux, H.; Georgatos, F. Management of an Academic HPC Cluster: The UL Experience. *Proceedings of the 2014 Intl. Conf. on High Performance Computing & Simulation (HPCS 2014), Bologna, Italy, July 2014*; 2014; pp 959−967.
(32) Weigend, F.; Ahlrichs, R. Balanced Basis Sets of Split Valence, Triple Zeta Valence and Quadruple Zeta Valence Quality for H to Rn: Design and Assessment of Accuracy. *Phys. Chem. Chem. Phys.* **2005**, *7*, 3297−3305.
(33) Weigend, F. Accurate Coulomb-Fitting Basis Sets for H to Rn. *Phys. Chem. Chem. Phys.* **2006**, *8*, 1057−1065.
(34) Grimme, S.; Ehrlich, S.; Goerigk, L. Effect of the Damping Function in Dispersion Corrected Density Functional Theory. *J. Comput. Chem.* **2011**, *32*, 1456−1465.
(35) Grimme, S.; Antony, J.; Ehrlich, S.; Krieg, H. A Consistent and Accurate Ab Initio Parametrization of Density Functional Dispersion Correction (DFT-D) for the 94 Elements H-Pu. *J. Chem. Phys.* **2010**, *132*, 154104.
(36) Loyer, F.; Bulou, S.; Choquet, P.; Boscher, N. D. Pulsed Plasma Initiated Chemical Vapor Deposition (PiCVD) of Polymer Layers− A Kinetic Model for the Description of Gas Phase to Surface Interactions in Pulsed Plasma Discharges. *Plasma Processes Polym.* **2018**, *15*, 1800121.
(37) Chen, N.; Reeja-Jayan, B.; Liu, A.; Lau, J.; Dunn, B.; Gleason, K. K. iCVD Cyclic Polysiloxane and Polysilazane as Nanoscale Thin-Film Electrolyte: Synthesis and Properties. *Macromol. Rapid Commun.* **2016**, *37*, 446−452.
(38) Kaltenbrunner, M.; Sekitani, T.; Reeder, J.; Yokota, T.; Kuribara, K.; Tokuhara, T.; Drack, M.; Schwödiauer, R.; Graz, I.; Bauer-Gogonea, S.; Bauer, S.; Someya, T. An Ultra-Lightweight Design for Imperceptible Plastic Electronics. *Nature* **2013**, *499*, 458−465.
(39) Atkins, P.; De Paula, J.; Keeler, J. *Atkins' Physical Chemistry*; Oxford University Press: 2018; p 908.
(40) Werner, F.; Siebentritt, S. Buffer Layers, Defects, and the Capacitance Step in the Admittance Spectrum of a Thin-Film Solar Cell. *Phys. Rev. Appl.* **2018**, *9*, 057047.
(41) Trujillo, N. J.; Wu, Q.; Gleason, K. K. Ultralow Dielectric Constant Tetravinyltetramethylcyclotetrasiloxane Films Deposited by Initiated Chemical Vapor Deposition (iCVD). *Adv. Funct. Mater.* **2010**, *20*, 607−616.
(42) Tu, H. E.; Su, C. J.; Jeng, U. S.; Leu, J. Pore Morphology of Low-k SiCxNy Films Prepared with a Cyclic Silazane Precursor Using Plasma-Enhanced Chemical Vapor Deposition. *Thin Solid Films* **2015**, *590*, 1−6.
(43) Boscher, N. D.; Choquet, P.; Duday, D.; Verdier, S. Chemical compositions of organosilicon thin films deposited on aluminium foil by atmospheric pressure dielectric barrier discharge and their electrochemical behavior. *Surf. Coat. Technol.* **2010**, *205*, 2438−2448.
(44) Tu, H.-E.; Chen, Y.-H.; Leu, J. Low-k SiCxNy Films Prepared by Plasma-Enhanced Chemical Vapor Deposition Using 1,3,5-trimethyl-1,3,5-trivinylcyclotrisilazane Precursor. *J. Electrochem. Soc.* **2012**, *159*, G56.
(45) Bulou, S.; Le Brizoual, L.; Miska, P.; de Poucques, L.; Hugon, R.; Belmahi, M.; Bougdira, J. The influence of CH4 addition on composition, structure and optical characteristics of SiCN thin films deposited in a CH_4/N_2/Ar/hexamethyldisilazane microwave plasma. *Thin Solid Films* **2011**, *520*, 245−250.

DOI: 10.1021/acsapm.9b00759
ACS Appl. Polym. Mater. 2019, 1, 3304−3312